Int J Biochem Mol Biol 2019;10(3):32-41
www.ijbmb.org /ISSN:2152-4114/IJBMB0097994

Original Article

Dependence of DNA looping on *Escherichia coli* culture density

Justin P Peters*, Vishwas N Rao, Nicole A Becker, L James Maher III

[1]*Department of Biochemistry and Molecular Biology, Mayo Clinic College of Medicine and Science, Rochester 55905, MN, USA; *Present address: Department of Chemistry and Biochemistry, University of Northern Iowa, Cedar Falls 50614, IA, USA.*

Received June 4, 2019; Accepted July 13, 2019; Epub August 15, 2019; Published August 30, 2019

Abstract: Repression of a promoter by entrapment within a tightly bent DNA loop is a common mechanism of gene regulation in bacteria. Besides the mechanical properties of the looped DNA and affinity of the protein that anchors the loop, cellular energetics and DNA negative supercoiling are likely factors determining the stability of the repression loop. *E. coli* cells undergo numerous highly regulated and dynamic transitions as resources are depleted during bacterial growth. We hypothesized that the probability of DNA looping depends on the growth status of the *E. coli* culture. We utilized a well-characterized repression loop model assembled from elements of the *lac* operon to measure loop length-dependent repression at three different culture densities. Remarkably, even with changes in supercoiling, there exists a dynamic compensation in which the contribution of DNA looping to gene repression remains essentially constant.

Keywords: DNA looping, DNA topology, lac repressor, growth phase, supercoiling

Introduction

Escherichia coli provides the basic paradigm for understanding gene regulation. We have focused on understanding repression of the *lac* promoter by formation of a tightly bent DNA loop anchored by Lac repressor (LacI) [1-3]. DNA looping dependence on growth status has not been studied. *E. coli* morphology, physiology, and cellular composition change through successive growth stages, as if the organism "differentiates" as a function of culture density. For example, the dimeric histone-like protein HU is present at ~30,000 copies per cell during exponential growth, but only ~15,000 in stationary phase [4]. Many nucleoid-associated proteins (NAPs) display similar growth-dependent changes in expression, and the resulting changes in nucleoid architecture and composition can profoundly impact global gene expression [5].

The superhelical density (σ_{total}) of the *E. coli* chromosome is usually -0.05 to -0.07 [4]. NAPs and other DNA-binding proteins can constrain supercoils, altering the level of unrestrained DNA supercoiling to about half of its intrinsic value [4]. Changing the expression of topoisomerase I (encoded by *topA*) or gyrase (encoded by *gyrA* and *gyrB*) can alter unrestrained supercoiling 2-fold and total supercoiling 30% [3, 6]. Supercoiling is also influenced at the local level by the activities of DNA and RNA polymerases [5, 6]. In vitro studies have demonstrated that DNA supercoiling promotes protein-mediated DNA looping [7] and modulates gene regulation [8].

The nucleoid compacts as *E. coli* enters stationary phase, DNA superhelical density decreases, and there is a general decrease in transcription and translation [5, 6]. Consequently, cells in stationary phase are strikingly distinct from their predecessors. What about the stability of DNA repression loops? Here we utilized a well-characterized episomal repression loop model to investigate the relationship between culture density and DNA supercoiling in determining the probability of DNA looping in an engineered switch. We hypothesized that looping probabili-

ty would depend on the degree of supercoiling, decreasing with deceasing supercoiling during culture growth. Remarkably, this was not observed.

Materials and methods

Growth curve assays

Overnight cultures of WT or ΔHU strains (see Supplementary Methods and Table S1) were diluted 10,000-fold into fresh medium in baffled Fernbach flasks and cultivated in a floor incubator shaker (250 rpm) at 37°C. Optical density was monitored at wavelength 600 nm every ~30 min for 24 h using a SpectraMax Microplate Reader. The starting inoculum and negative control (medium without bacteria) had similar OD_{600} levels (<0.1), and this value was subtracted from each reading. As necessary, dilutions were performed just prior to reading so OD_{600} did not exceed ~0.5. From a modified Gompertz equation [9]:

$$OD_{600}(t) = Ae^{-e\left(\frac{\mu_{max}e}{A}(L-t)+1\right)}$$

growth (optical density, OD) as a function of time (t) where A, the growth asymptote, μ_{max}, the maximum specific growth rate, and L, the lag time, were fitted (**Table 1** and Figure S1).

Chloroquine gel analysis of DNA supercoiling

pUC19 topoisomers (~600 ng) were separated by electrophoresis through 1% agarose slab gels (16 cm × 13 cm) containing 0-6 μg/mL chloroquine. Separation was at 2.5 V/cm for 17 h at 4°C in 1X TAE buffer (40 mM Tris-acetate, pH 8.3 with 1 mM EDTA) containing chloroquine diluted from 1 mg/mL stock. Gels were incubated for 1 h in buffer containing 0.5 μg/mL ethidium bromide. Images were recorded on a Typhoon FLA7000 imager.

Here, we employ the practice of estimating chromosomal supercoiling density from the plasmid population. The assumption is that the mean chromosomal supercoiling status mirrors the plasmid average if the distribution of topoisomers is tight and appears normally distributed.

Superhelical density $\sigma = \Delta Lk/Lk_0$ (**Table 2**) is defined as ΔLk, the linking number deficit divided by Lk_0, the linking number of the relaxed plasmid. For pUC19, Lk_0 = 255.8, the number of base pairs (2,686) divided by the assumed helical repeat (10.5 bp/turn). We determined ΔLk for each sample and chloroquine concentration by band counting from the most abundant topoisomer relative to the most abundant topoisomer in the lane corresponding to OD_{600} = 1, for which ΔLk = -14 from two-dimensional gel analysis (see Supplementary Methods and Figure S2).

β-galactosidase activity assays

β-galactosidase activity was determined using a colorimetric enzyme assay performed either from a batch culture on aliquots in 2-mL tubes or using high-throughput methodology. Both methods gave comparable results. For the high-throughput method, triplicate 1.1-mL subcultures with or without 2 mM isopropyl β-D-1-thiogalactopyranoside (IPTG) were grown at 37°C until a predetermined OD_{600} value in 96 deep-well round bottom plates that were inoculated with 30 μL saturated overnight culture. Lysis of 100 μL of each subculture in 900-μL Z-buffer (60 mM Na_2HPO_4, 40 mM NaH_2PO_4, 10 mM KCl, 1 mM $MgSO_4$, 50 mM β-mercaptoethanol) occurred with 50 μL chloroform and 50 μL 0.1% SDS, followed by vortex agitation for 10 s. Samples were equilibrated at 30°C for 5 min, followed by the addition of 200-μL O-nitrophenylpyranogalactoside (ONPG; 4 mg/mL) in Z-buffer. Incubation continued at 30°C with accurate timing until OD_{420} reached ~0.5. Reactions were terminated by addition of 500 μL of 1 M Na_2CO_3 and reaction times recorded. Cell debris was removed by centrifugation for 3 min at 15,000 × g. Optical densities were measured with SpectraMax Microplate Reader. β-galactosidase activity (E, Miller Units) was calculated according to:

$$E = 1000\left(\frac{OD_{420} - 1.75 \cdot OD_{550}}{t \cdot v \cdot OD_{600}}\right)$$

where OD_λ is optical density at wavelength λ, t indicates reaction time (min), and v represents assay culture volume (mL). Assays were performed with a minimum of 3 colonies repeated on at least 2 days. For the batch method and thermodynamic modeling, see Supplementary Methods.

The repression level is given by the ratio of E from the induced construct incapable of looping (full activity) to any looping construct: $E_{02+IPTG}/E_{construct}$. Looping contribution is defined

Table 1. Parameters from modified Gompertz fits of growth data[a]

Parameter	Description	WT cells	ΔHU cells
A	growth asymptote (OD_{600})	2.64 (0.18)	2.43 (0.18)
μ_{max}	maximum specific growth rate (min^{-1})	0.00668 (0.00136)	0.00577 (0.00119)
L	lag time (min)	175.32 (37.93)	177.74 (40.46)

[a]The range of a 95% confidence interval is indicated in parenthesis.

Table 2. Total DNA supercoiling

Growth point	OD_{600} Target	WT σ_{total}	ΔHU σ_{total}
1	0.01	-0.059	-0.055
2	0.1	-0.059	-0.051
3	0.5	-0.055	-0.051
4	1.0	-0.055[a]	-0.051
5	1.5	-0.051	-0.047
6	early stationary (2.5 WT, 2.0 ΔHU)	-0.047	-0.043
7	late stationary (2.5 WT, 2.0 ΔHU)	-0.047	-0.043

[a]Determined from two-dimensional analysis.

-IPTG ($E_{O2\text{-}IPTG}/E_{Osym\text{-}O2\text{-}IPTG}$) or +IPTG ($E_{O2+IPTG}/E_{Osym\text{-}O2+IPTG}$) to account for any growth-dependent changes in that IPTG condition.

Results and discussion

E. coli growth curves and superhelical density

Growth of wild-type *E. coli* (WT) in rich media was monitored (**Figure 1A**). To guide the eye, these and subsequent plots were divided into early, middle, and late growth/stationary. Growth data were fit with a modified Gompertz growth model (**Table 1**). We observed lower maximal specific growth rate and lower culture density plateau (**Figure 1B** and **Table 1**) in a strain with chromosomal deletions of both *hupA* and *hupB* genes (ΔHU), which is known to support less DNA looping [1, 2].

Growth points were chosen to investigate DNA supercoiling and DNA looping (**Figure 1C** and **1D**, arrows). We isolated pUC19 plasmid from WT cells and separated topoisomers by gel electrophoresis with chloroquine ranging from 1 μg/mL to 6 μg/mL (**Figure 1E-H**). Growth point 4 (OD_{600} = 1) plasmid was spiked into a distribution of relaxed topoisomers (see Supplementary Methods) and two-dimensional gel electrophoresis performed (**Figure 1I**) to determine ΔLk (-14) and σ_{total} (**Table 2**), serving as a reference for other lanes. The estimated σ_{total} (-0.055) was consistent with previous measurements [4]. This method showed a monotonically decreasing level of total supercoiling (**Table 2**). pUC19 plasmid from ΔHU cells separated by gel electrophoresis with 4 μg/mL or 6 μg/mL chloroquine (**Figure 1J** and **1K**) also showed decreasing σ_{total} as culture density increased (**Table 2**). Additionally, total DNA supercoiling was lower in ΔHU cells than WT cells at every culture density, consistent with previous studies [1, 4]. Together, these results showed that total DNA supercoiling decreased with culture density.

We next examined unrestrained (diffusible) DNA supercoiling using superoil-dependent promoters as previously described [3, 6]. Unrestrained supercoiling followed a similar pattern as total supercoiling (Figure S3), progressing from relaxed (early) to more supercoiled (middle) to relaxed (stationary). Unrestrained supercoiling was greater in the ΔHU strain, consistent with the role of HU as a histone-like protein that constrains supercoils [4].

Culture density dependence of DNA looping

We hypothesized that DNA looping would be facilitated in the growth phase with most supercoiled DNA. We utilized a previously characterized engineered episomal system containing elements of the *lac* operon with a β-galactosidase (*lacZ*) reporter (**Figure 2A** and **2B**). Looping constructs contained a strong distal O_{sym} operator (red) separated from a weak proximal O_2 operator (blue) by 63.5 bp to 90.5 bp center-to-center (**Figure 2C**). O_2 normally present within the *lacZ*-coding region was destroyed by site-directed mutagenesis.

The weaker O_2 binding site overlaps with the promoter of the *lacZ* reporter. Repression is strongly enhanced by placement of high-affinity

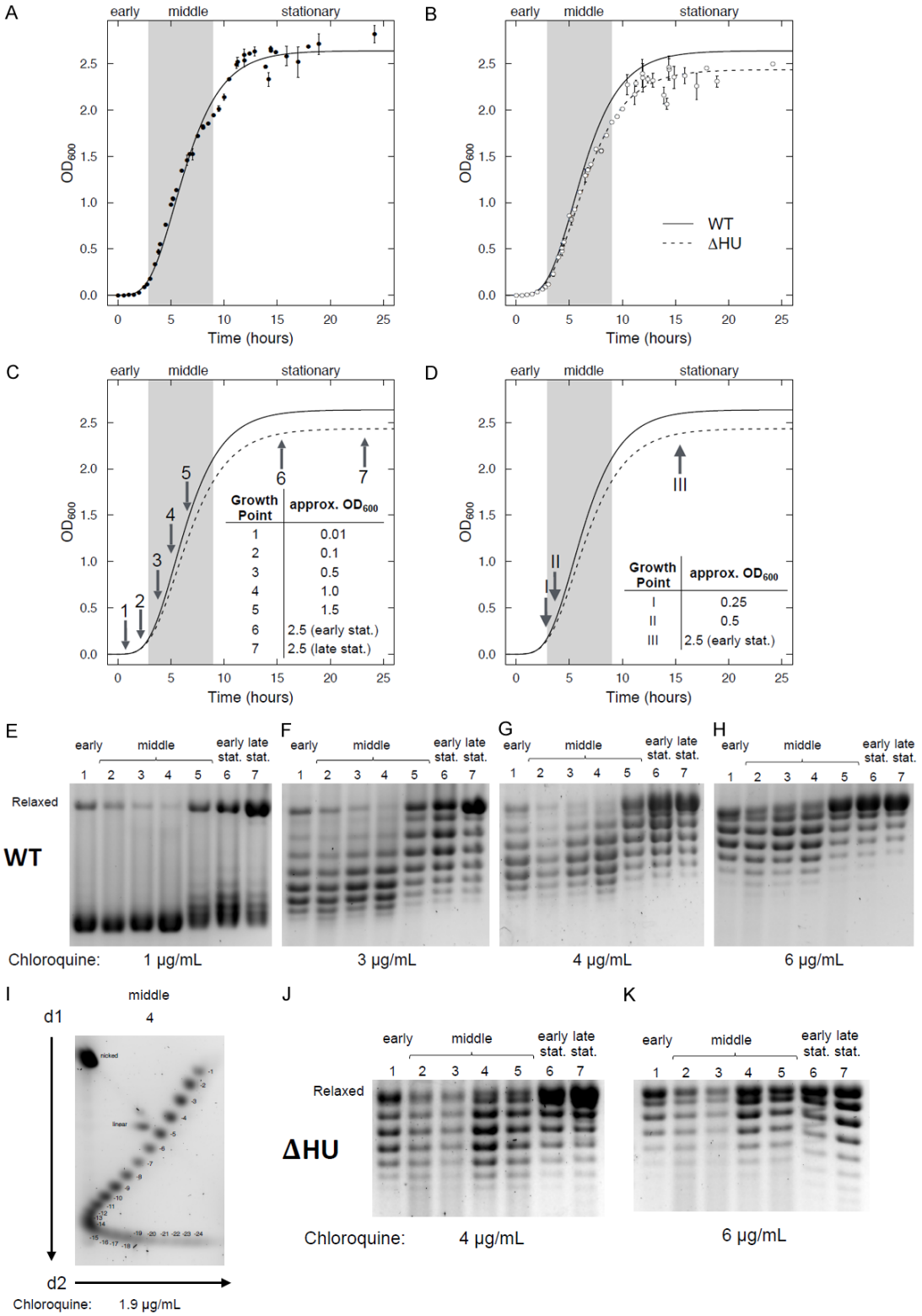

Figure 1. *E. coli* growth curves and total DNA supercoiling. (A) WT *E. coli* growth curve showing the three main growth phases. Growth data (error bars indicating standard deviation) were fit using a modified Gompertz growth model [9]. (B) Comparison growth curve in a strain with chromosomal deletions in both *hupA* and *hupB* genes (ΔHU). Growth points (arrows) in supercoiling (C) and looping (D) assays. pUC19 was isolated from WT cells and separated by gel electrophoresis with chloroquine concentrations of (E) 1 μg/mL, (F) 3 μg/mL, (G) 4 μg/mL, or (H) 6 μg/mL. Two-dimensional gel electrophoresis performed on growth point 4 (I) determined the change in linking number (-14) which served as a reference. pUC19 from ΔHU cells was separated by gel electrophoresis with (J) 4 μg/mL or (K) 6 μg/mL chloroquine.

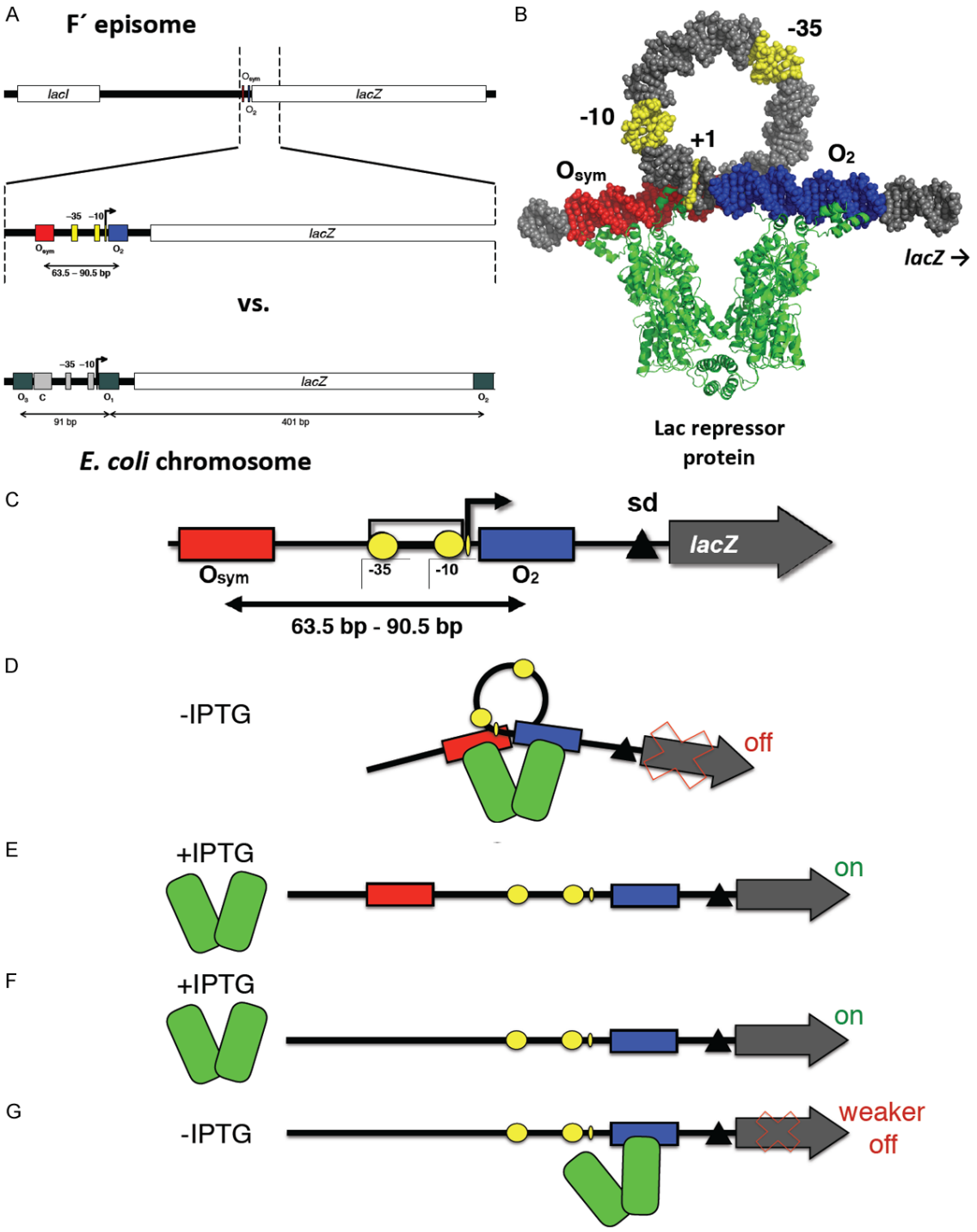

Figure 2. DNA looping system. (A) Engineered *lacI* gene through the *lacZYA* genes was placed on the single copy F128 episome (top). In contrast, endogenous *lac* promoter including the start of the *lacZ* gene (bottom) contains three operators (dark gray) separated center-to-center by 91 bp and 401 bp, a catabolite activator binding site (gray, C), transcription start site (broken arrow) and -10 and -35 promoter elements (gray). (B) Schematic rendering of one possible geometry of a 78.5-bp repression loop with tetrameric repressor protein (LacI, PDB code 1Z04) in green. (C) DNA looping constructs contain a strong distal O_{sym} operator (red) separated center-to-center from a weak proximal O_2 operator (blue) by 63.5 bp to 90.5 bp. Other cis elements are the transcription start site (broken arrow), -10 and -35 elements (yellow) of the *lacUV5* promoter (boxed), Shine-Dalgarno sequence (black triangle), and *lacZ* gene (gray arrow). (D) Without IPTG, DNA looping results in lower β-galactosidase activity. (E) With IPTG, LacI is released in an allosteric manner, thereby allowing higher β-galactosidase activity. (F) Control construct lacking distal O_{sym} operator (therefore incapable of looping) was used for normalization. (G) Weak residual repression from steric occlusion is detected from the control construct without IPTG.

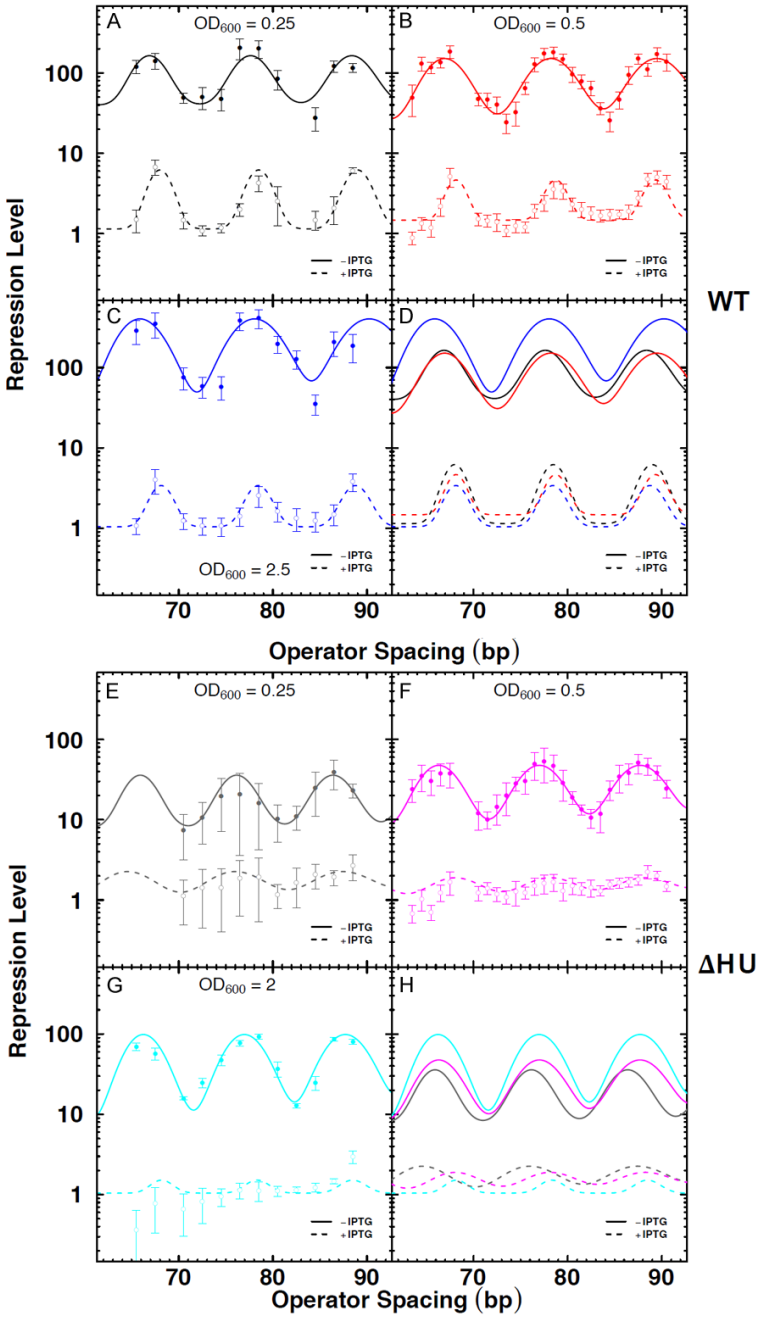

Figure 3. β-galactosidase activity assay of DNA looping in WT and ΔHU cells. Repression level for WT cells at (A) OD_{600} = 0.25 (black), (B) OD_{600} = 0.5 (red), and (C) OD_{600} = 2.5 (blue). (D) Overlay of WT plots. Repression level for ΔHU cells at (E) OD_{600} = 0.25 (gray), (F) OD_{600} = 0.5 (magenta), and (G) OD_{600} = 2.0 (cyan). (H) Overlay of ΔHU plots. Data (error bars indicating standard deviation) were fit using a thermodynamic model described previously [10]. Data at OD_{600} = 0.5 previously published for WT and ΔHU cells [2].

O_{sym} upstream of the promoter, since LacI tetramer binding at O_{sym} has the potential to increase the local repressor concentration at O_2 by virtue of DNA looping. Without the allolactose analog IPTG, LacI binds the two operators forming a DNA loop that sequesters the *lacUV5* promoter and represses *lacZ* expression (**Figure 2D**). With IPTG inducer, LacI is substantially released from the DNA operators in an allosteric manner, allowing higher *lacZ* expression (**Figure 2E**). A construct lacking O_{sym}, therefore incapable of looping, serves as a normalization control (**Figure 2F**). *lacZ* is only weakly repressed with O_2 present in isolation (**Figure 2G**).

We performed β-galactosidase activity (*E*) assays of DNA looping in WT cells (**Figure 1D**, arrows) grown plus and minus IPTG. Repression level was calculated (see Methods and **Figure 3**) and fit using a thermodynamic model (**Table 3**) described previously [10]. New data were collected for OD_{600} = 0.25 (**Figure 3A**) and OD_{600} = 2.5 (**Figure 3C**), while OD_{600} = 0.5 (**Figure 3B**) were previously reported [2]. The model is overlaid at three growth points in **Figure 3D**.

As expected, the sinusoidal pattern revealed the twist stiffness of DNA (C_{app} in **Table 3**) that persisted with inducer (indicating weak residual looping) and overall was of lower magnitude than in vitro measurements [1, 2]. Unexpectedly, given that supercoiling decreased in stationary phase, helical repeat (*hr*) increased from 10.76 bp/turn to 12.18 bp/turn (-IPTG, **Table 3**). For +IPTG, *hr* remained less than 10.6 bp/turn with a pattern more consistent with the changes in supercoiling. Additionally, $sp_{optimal}$ followed a pattern of increase then decrease that is consistent with the measured changes in supercoiling. The values were systematically higher for +IPTG than -IPTG (**Table 3**), which likely reflects the mentioned differences in *hr* and

Table 3. Parameters from thermodynamic model fits of repression level data[a]

Inducer status	*hr*[b]	C_{app}[c]	K_{max}[d]	K_{NSL}[e]	$sp_{optimal}$[f]	K_{O2}[g]
OD_{600} = 0.25, WT						
-IPTG	10.76 (1.38)	*0.99 (1.29)*	124.70 (57.77)	*35.29 (38.10)*	77.63 (0.92)	3.14
+IPTG	10.49 (0.52)	1.90 (0.69)	5.06 (0.75)	*0.14 (0.31)*	78.49 (0.33)	0
OD_{600} = 0.25, ΔHU						
-IPTG	10.24 (2.25)	0.90 (0.44)	28.04 (13.29)	2.97 (1.80)	76.15 (2.46)	0.01
+IPTG	11.42 (8.28)	*0.45 (2.26)*	*1.26 (5.07)*	*0 (5.06)*	76.00 (6.57)	0
OD_{600} = 0.5, WT						
-IPTG	11.27 (0.54)	0.70 (0.31)	145.82 (22.97)	*22.36 (22.21)*	78.21 (0.41)	2.45
+IPTG	10.59 (0.66)	2.63 (3.64)	3.61 (1.95)	0.53 (0.33)	78.74 (0.57)	0.13
OD_{600} = 0.5, ΔHU						
-IPTG	10.70 (1.19)	*0.65 (1.13)*	59.26 (35.73)	*6.01 (38.95)*	77.00 (0.73)	3.21
+IPTG	10.10 (2.49)	*0.38 (0.45)*	*1.30 (1.34)*	*0 (1.61)*	78.16 (1.74)	0.46
OD_{600} = 2.5, WT						
-IPTG	12.18 (1.29)	0.64 (0.52)	386.54 (139.09)	*10.50 (114.15)*	78.06 (0.74)	6.05
+IPTG	10.32 (0.80)	1.90 (1.15)	2.36 (1.28)	*0.04 (0.25)*	78.45 (0.76)	0
OD_{600} = 2.0, ΔHU						
-IPTG	10.73 (0.21)	0.72 (0.04)	253.18 (7.98)	*2.29 (8.63)*	76.97 (0.06)	14.08
+IPTG	10.15 (2.25)	1.90 (1.60)	1.30 (0.77)	*0.12 (0.22)*	78.32 (1.79)	1.74

[a]Data at OD_{600} = 0.5 previously published for WT and ΔHU cells [2]. The range of a 95% confidence interval is indicated in parenthesis. Parameters not well determined by fitting are indicated in italics. [b]DNA helical repeat (bp/turn). [c]Apparent DNA torsional modulus (× 10^{-19} erg-cm). [d]Equilibrium association constant for looped state with maximal stability. [e]Equilibrium association constant for non-specific looped state. [f]Optimal spacing (near 77 bp in the interval tested) for most stable loop. [g]Equilibrium association constant for single operator bound state was determined experimentally.

number of turns need to produce a phased loop. Surprisingly, -IPTG data showed that repression level increased (from a mean of 97.6 to 184.6) as culture density increased, while the opposite trend was observed +IPTG, where repression level decreased (from a mean of 2.6 to 1.8). **Table 3** captures this trend as increasing K_{max} for WT cells -IPTG, but decreasing K_{max} for WT cells +IPTG. Only this second result was consistent with our hypothesis, and unexpectedly -IPTG and +IPTG showed opposite trends. We wondered if such trends were unique to WT cells.

We therefore performed β-galactosidase activity assays for ΔHU cells ± IPTG. Again, new data were collected for OD_{600} = 0.25 (**Figure 3E**) and OD_{600} = 2.0 (**Figure 3G**), OD_{600} = 0.5 (**Figure 3F**) was previously reported [2], repression level data were fit using the thermodynamic model (**Table 3**), and the model results overlaid in **Figure 3H**. ΔHU repression levels were consistently ~3-fold lower than WT, as expected [2]. This manifested as ~3-fold decrease in K_{max} and K_{NSL}. Similar to WT trends, for ΔHU cells K_{max} increased -IPTG but was essentially unchanged +IPTG, and repression level -IPTG increased (from a mean of 16.8 to 48.7), whereas +IPTG decreased (from a mean of 1.7 to 1.1). These results suggested that looping improved in stationary phase, which was contrary to our hypothesis of supercoiling as a primary facilitator of DNA looping.

What might explain this apparent enhanced looping in stationary phase? One hint came from the trend for K_{O2}. As culture density increased, K_{O2} increased for ΔHU cells ±IPTG, with this trend was less pronounced for WT cells (**Table 3**). This observation suggested that as culture density increased, LacI binding to O_2 increased even in the absence of looping.

Culture density effects independent of DNA looping

We therefore sought to clarify gene regulation effects independent of DNA looping. We performed β-galactosidase activity assays for the control construct with no looping possible (**Figure 2F** and **2G**), collecting data throughout the entire OD_{600} range (**Figure 4A-C**). From WT

cells -IPTG, we seeded fresh cultures -IPTG (**Figure 4A**, blue) or +IPTG (**Figure 4B**, blue). Lines have been drawn to guide the eye. The repression level data (**Figure 4C**, blue) revealed an intriguing growth dependence: repression level -IPTG increased from ~2 early to ~4 during middle growth, in agreement with previous observations made during maximal growth [1, 2]. However, in stationary phase repression level roughly doubled again (**Figure 4C**, blue). This finding was consistent with our earlier observation of increased looping-*independent* repression at later growth stages. To understand the basis of this observation, we examined $E_{\text{-IPTG}}$ and $E_{\text{+IPTG}}$ more closely. $E_{\text{-IPTG}}$ displayed minor increase throughout growth (**Figure 4A**, blue and inset), whereas $E_{\text{+IPTG}}$ displayed robust increase from early into stationary phase (**Figure 4B**, blue). This peculiar result can be explained by the dual role of LacI in blocking transcriptional initiation when uninduced and increasing RNA polymerase promoter affinity through cooperative interactions to increase the rate of the first round of productive transcription when induced [11]. Effectively, by setting the trigger the system can respond rapidly to the release of repression with increased transcription.

To verify that this result was due to functional LacI, we used a mutant strain (LacI Y282D) impaired in tetramer assembly. The Y282D mutant has poor affinity for operators although it still binds IPTG similarly [12]. $E_{\text{-IPTG}}$ and $E_{\text{+IPTG}}$ were both fairly constant (**Figure 4A** and **4B**, green), with a hint that expression was inversely dependent on specific growth rate (c.f. the behavior observed in Figure S1A), resulting in repression level values near one across the entire OD_{600} range (**Figure 4C**, green). Therefore, the observed $E_{\text{+IPTG}}$ increase required functional LacI.

To better understand how looping-independent effects influenced DNA looping, we examined the ~78 bp spacing in detail (**Figure 4D-F**). Data for the mutant strain (LacI Y282D) revealed that expression increases in a similar manner for both $E_{\text{-IPTG}}$ (**Figure 4D**, magenta) and $E_{\text{+IPTG}}$ (**Figure 4E**, magenta), resulting in low repression level values across the entire OD_{600} range (**Figure 4F**, magenta and inset). For WT LacI, $E_{\text{-IPTG}}$ remained low throughout (**Figure 4D**, black and inset), consistent with looping-dependent repression. In contrast, $E_{\text{+IPTG}}$ displayed low initial values that steadily rose into stationary phase (**Figure 4E**, black). As a result, repression level values -IPTG steadily rose (**Figure 4F**, solid black line) versus +IPTG, where there was a slight decrease (**Figure 4F**, dashed black line and inset). Thus, the surprising finding shown in **Figure 3** and recapitulated for this spacing resulted from the repression level normalization construct itself being dependent on culture density.

DNA looping contribution to repression

Lastly, for each IPTG condition we calculated a looping contribution (see Methods) for the 78.5 bp spacing, which avoided the aforementioned normalization issue. Lines have been drawn to guide the eye and for simplicity, only the three data points from **Figure 3** have been shown (**Figure 4G**, gray open squares). Looping contribution remained relatively constant across growth phases but was obviously much greater -IPTG than +IPTG (roughly 60-fold versus 4-fold, respectively). Since 78.5 bp was near sp_{optimal}, we also used the thermodynamic model (**Table 3**) to calculate an apparent K_{max} that accounts for the changing K_{O2}, $K°_{max} = K_{max}/K_{O2}$. We observed relatively constant $K°_{max}$ (54.4 average) during growth for WT cells -IPTG. This parameter became less reliable for cases when K_{O2} is near zero, as is typical for +IPTG.

Finally, the looping contribution over residual looping (IPTG induced) provided an estimate of the fold repression attributed to specific looping from uninduced LacI (**Figure 4H**). Strikingly, this ~15-fold repression is remarkably constant across growth phases despite the fact that many cell parameters (e.g. DNA supercoiling) are changing during this time. Looping contribution over residual looping was comparable for the ΔHU strain (**Figure 4H**, gray open squares), even though each looping contribution was lower for this strain. This result was also unexpected; the ratio of two attenuated values happened to remain constant. Using the thermodynamic model for the two cases where $K°_{max}$ can be reliably calculated from the ΔHU data (**Table 3**), we calculated an average value of 18.2 (which in practice does not need correction for residual looping +IPTG, since this value is near one). Thus, many complex competing factors balanced yielding an unexpectedly consistent repression contribution from looping.

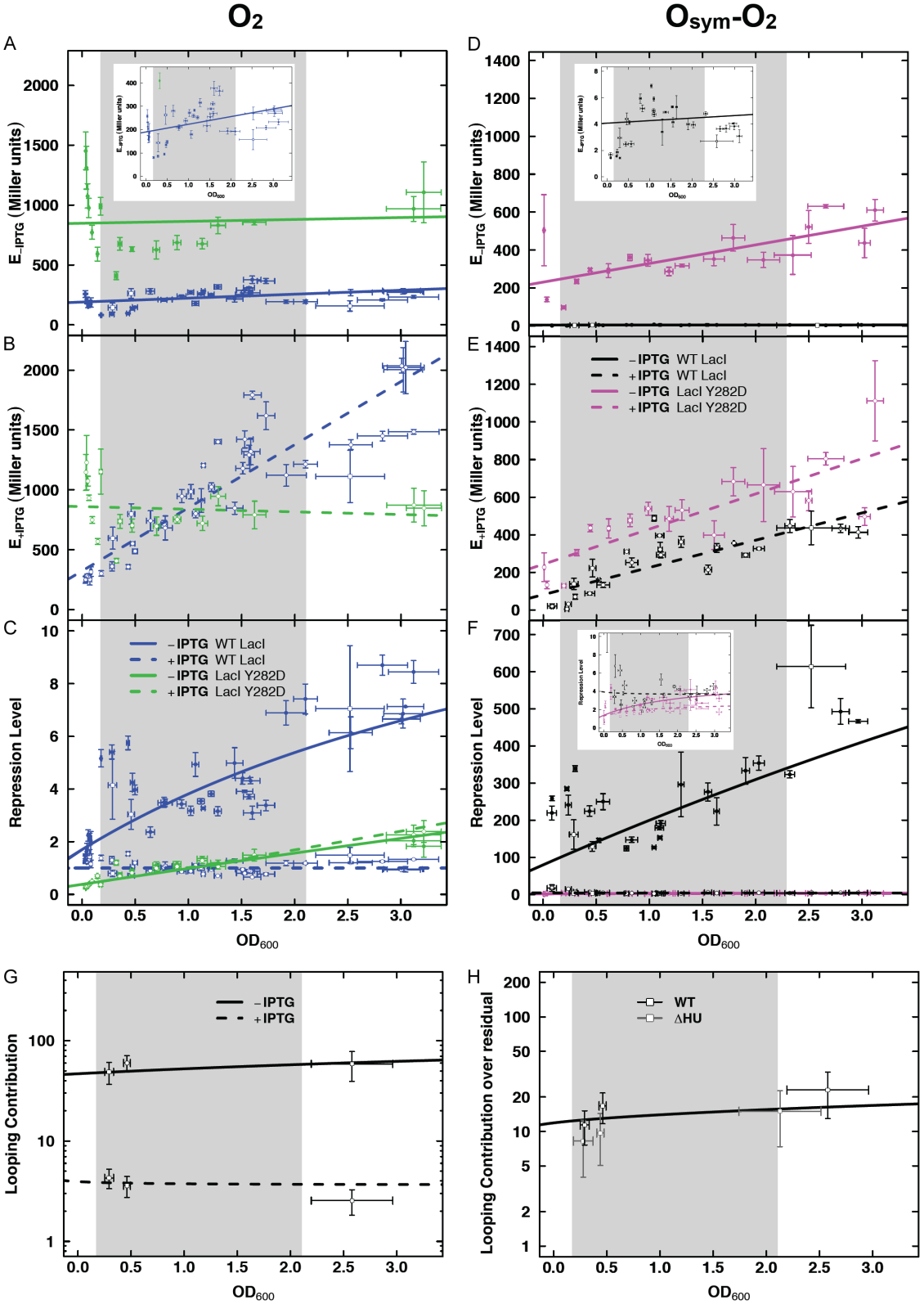

Figure 4. Summary for the ~78 bp operator spacing. β-galactosidase activity assays from cultures expressing either wild-type repressor protein (WT LacI, blue or black) or a mutant impaired in tetramer assembly (LacI Y282D, green or magenta). Single operator (O_2) data as a function of OD_{600} (A) E_{-IPTG}, (B) E_{+IPTG}, or (C) repression level. Double operator (O_{sym}-O_2) data as a function of OD_{600} for the 78.5 bp spacing construct (D) E_{-IPTG}, (E) E_{+IPTG}, or (F) repression level. The looping contribution to repression (G) was calculated for -IPTG or +IPTG. Residual looping in 2 mM IPTG appeared as looping contribution greater than one, which was factored out in the looping contribution over residual looping (H). Open squares show data taken from **Figure 3**. Error bars indicate standard deviation. Lines are drawn to guide the eye.

Summary

This work tested the hypothesis that DNA looping depends on *E. coli* culture density. We proposed that DNA supercoiling status would be the major determinant of DNA looping. This hypothesis proved too simplistic. Instead, among the numerous changes during stationary phase (including decreased supercoiling) we observed sustained repression. Several important themes emerged from our analysis. First, the level of repression for ΔHU was always impaired relative to WT, regardless of growth status. Second, β-galactosidase activity +IPTG was not constant throughout growth, even in the absence of DNA looping. However, after accounting for this bizarre variable, the contribution of DNA looping to gene repression was strikingly consistent. The dynamic balance that evolved to conserve the contribution of DNA looping is a remarkable adaptation. As a clear precedent, Record and co-workers showed that protein-DNA interactions in *E. coli* are preserved by compensating effects when the internal ionic strength is altered [13].

Acknowledgements

We thank Lauren Mogil for technical assistance. This work was supported by the Mayo Foundation and the National Institutes of Health (GM75965 to LJM).

Disclosure of conflict of interest

None.

Address correspondence to: L James Maher III, Department of Biochemistry and Molecular Biology, Mayo Clinic College of Medicine and Science, 200 First St. SW, Rochester, 55905, MN, USA. Tel: 507-284-9041; Fax: 507-284-2053; E-mail: maher@mayo.edu

References

[1] Becker NA, Kahn JD and Maher LJ 3rd. Bacterial repression loops require enhanced DNA flexibility. J Mol Biol 2005; 349: 716-730.

[2] Becker NA, Kahn JD and Maher LJ 3rd. Effects of nucleoid proteins on DNA repression loop formation in Escherichia coli. Nucleic Acids Res 2007; 35: 3988-4000.

[3] Mogil LS, Becker NA and Maher LJ 3rd. Supercoiling effects on short-range DNA looping in E. coli. PLoS One 2016; 11: e0165306.

[4] Higgins NP and Vologodskii AV. Topological behavior of plasmid DNA. Microbiol Spectr 2015; 3.

[5] Dillon SC and Dorman CJ. Bacterial nucleoid-associated proteins, nucleoid structure and gene expression. Nat Rev Microbiol 2010; 8: 185-195.

[6] Abu Mraheil M, Heisig A and Heisig P. An improved assay for the detection of alterations in bacterial DNA supercoiling in vivo. Pharmazie 2013; 68: 541-548.

[7] Yan Y, Leng F, Finzi L and Dunlap D. Protein-mediated looping of DNA under tension requires supercoiling. Nucleic Acids Res 2018; 46: 2370-2379.

[8] Finzi L and Dunlap D. Supercoiling biases the formation of loops involved in gene regulation. Biophys Rev 2016; 8 Suppl 1: 65-74.

[9] Zwietering MH, Jongenburger I, Rombouts FM and van 't Riet K. Modeling of the bacterial growth curve. Appl Environ Microbiol 1990; 56: 1875-1881.

[10] Peters JP, Becker NA, Rueter EM, Bajzer Z, Kahn JD and Maher LJ 3rd. Quantitative methods for measuring DNA flexibility in vitro and in vivo. Methods Enzymol 2011; 488: 287-335.

[11] Straney SB and Crothers DM. Lac repressor is a transient gene-activating protein. Cell 1987; 51: 699-707.

[12] Daly TJ and Matthews KS. Characterization and modification of a monomeric mutant of the lactose repressor protein. Biochemistry 1986; 25: 5474-5478.

[13] Richey B, Cayley DS, Mossing MC, Kolka C, Anderson CF, Farrar TC and Record MT Jr. Variability of the intracellular ionic environment of Escherichia coli. Differences between in vitro and in vivo effects of ion concentrations on protein-DNA interactions and gene expression. J Biol Chem 1987; 262: 7157-7164.

Supplementary Methods

Bacterial strains

This work was performed using *E. coli* strain FW102 (WT; [1]) or an isogeneic strain in which the endogenous *hupA* and *hupB* genes encoding HU protein were disrupted (ΔHU) [2, 3]. DNA looping constructs driving the *lacZ* reporter were moved from plasmids into the large, single copy F128 episome by homologous recombination. F128 also encoded either the *lacI* gene producing wild type levels of lac repressor (WT LacI) or a LacI monomer incapable of tight DNA binding or repression (LacI Y282D; [4]). Bacterial conjugation and selection for the desired recombinants were carried out as described [1]. After bacterial mating and selection, correct recombinants were confirmed by PCR amplification and sequence analysis [3].

Plasmid isolation

WT or ΔHU strains were transformed with plasmid pUC19 and grown overnight. Subcultures were grown to specified growth points, and plasmid was harvested using a Maxiprep kit (Qiagen). DNA concentration was determined by UV spectrophotometry using a Nanodrop 1000 (Thermo Scientific).

Topoisomerase I treatment

Purified pUC19 plasmids (~2 μg) were relaxed by *E. coli* topoisomerase I (Topo I, New England Biolabs) at 37°C for 40 min in CutSmart buffer containing 0-8 μg/mL of ethidium bromide (EtBr), to obtain topoisomers with superhelical densities varying over a wide range. Each reaction generated a Gaussian distribution of topoisomers about a mean, and the EtBr concentration determined the position of the mean (Figure S2). Reactions were then extracted twice with phenol/chloroform, once with chloroform, and precipitated from ethanol to remove EtBr and Topo I. From the intensities and positions of the distributions (Figure S2), a mixture of samples relaxed at different EtBr concentrations was generated with topoisomers of equal concentration and covering the entire range of interest. Together with an excess of sample from a culture at OD_{600} = 1, this mixture was used for the two-dimensional gel electrophoresis.

Two-dimensional gel electrophoresis

Approximately 2.5 μg of the spiked topoisomer mixture was loaded into a circular well in the corner of a 1% agarose slab gel (16 cm × 13 cm). Electrophoresis in the first dimension was at 3 V/cm for 24 h at 4°C in 1X TAE (40 mM Tris-acetate, pH 8.3 with 1 mM EDTA). The gel was then soaked in 1X TAE buffer containing 1.9 μg/mL chloroquine for 5 h. After rotating the gel by 90° clockwise, it was electrophoresed at 4°C in 1X TAE with 1.9 μg/mL chloroquine for 24 h at 2.5 V/cm. The gel was stained in a 1X SYBR Gold (Invitrogen) solution in running buffer overnight and destained overnight before imaging on a Typhoon FLA7000 imager (General Electric).

Luciferase assays

Luciferase reporter assays were performed, in which firefly *luc* expression is driven by the promoter cluster p_{topA} or promoter p_{gyrA} integrated into the F128 episome (Figure S3). Overnight cultures (1 mL, inoculated with individual colonies) of either WT or ΔHU cells (with the episomal *luc* reporters) were grown in Luria-Bertani media with appropriate antibiotics (Kan and Strep). Subcultures were grown to the predetermined growth points in 24 deep-well, round-bottom culture blocks shaking at 37°C. Samples (90 μL) were supplemented with 10 μL buffer (1 M K_2HPO_4, pH 7.8 and 20 mM EDTA) and incubated at -80°C for 30 min. Samples were then thawed at room temperature and incubated with 200 μL 1X luciferase cell culture lysis reagent (Promega) and 100 μL of a solution containing lysozyme (5 mg/mL) and BSA (5 mg/mL) for 10 min at room temperature. Lysates of precise volume (10 μL) were analyzed on a GloMax 96 microplate luminometer (Promega) with automated injection of 50 μL of luciferase assay reagent (Promega). Each sample was read in duplicate. Assays were performed for cultures derived from at least eight colonies for each independent strain and repeated on four different days.

The luminometer light units (LU) were corrected for sample volume (analyzed in microliters) and optical density at 600 nm.

β-galactosidase activity assays

For the batch method, 1 mL of overnight culture seeded two 50 mL subcultures, one of which contained 2 mM IPTG. Cells were grown in Erlenmeyer flasks at 37°C with shaking (250 rpm). At various time points, aliquots were simultaneously collected for OD_{600} reading and lysis. Cells were pelleted and placed on ice during the reading, then resuspended in 1 mL of Z-buffer (60 mM Na_2HPO_4, 40 mM NaH_2PO_4, 10 mM KCl, 1 mM $MgSO_4$, 50 mM β-mercaptoethanol). Cells were lysed by the addition of 50 μL chloroform and 50 μL 0.1% SDS followed by a 10-s pulse vortex. Samples were then equilibrated at 30°C for 5 min, followed by the addition of 200 μL of 4 mg/mL O-nitrophenylpyranogalactoside solution (ONPG) in Z-buffer. Incubation was continued at 30°C with accurate timing until OD_{420} reached ~0.5. Reactions were terminated with 500 μL of 1 M Na_2CO_3 and the reaction time recorded. Cell debris was removed by centrifugation for 3 min at 15,000 × g. Supernatant (350 μL) was then added to a clear 96 well micro-titer plate and sample absorbance was measured on a SpectraMax Microplate Reader (Molecular Devices). β-galactosidase activity (*E*) in Miller units was calculated as described:

$$E = 1000\left(\frac{OD_{420} - 1.75 \cdot OD_{550}}{t \cdot v \cdot OD_{600}}\right)$$

Thermodynamic modeling of DNA looping

The thermodynamic model described here is based on the premise that promoter repression is determined by the degree of occupancy of the proximal *lac* operator (O_2 in our system) by LacI at equilibrium [5-11]. Experimentally, the fraction of promoter bound by LacI is given by:

$$f_{bound} = \frac{\text{max induced activity} - \text{observed activity}}{\text{max induced activity}}$$

The theoretical f_{bound} is modeled as a function of DNA operator-to-operator spacing (*sp*), with five adjustable parameters: *hr*, C_{app}, K_{max}, K_{NSL} and $sp_{optimal}$ as follows:

$$f_{bound} = \frac{K_{SL} + K_{NSL} + K_{O_2}}{1 + K_{SL} + K_{NSL} + K_{O_2}}$$

where each of the association equilibrium constants absorbs the (assumed) constant cellular concentration of repressor and is therefore dimensionless. The equilibrium constant for the state of singly-bound repressor bound to the O_2 operator (relative to the state of free O_2 operator), K_{O2}, is experimentally determined from a control strain with an isolated O_2 operator. K_{NSL} is an adjustable parameter accounting for other possible repressed states than looping from O_{sym} (i.e. non-specific looping), and the association equilibrium constant for the specific looped state is given by:

$$K_{SL} = \sum_{i=-5}^{5} K_{max}\, e^{-(sp - sp_{optimal} + i \cdot hr)^2/(2\varphi_{Tw}^2)}$$

with *sp* is the actual spacing (bp) between operator O_{sym} and operator O_2 centers, $sp_{optimal}$ is the spacing (within the range tested) for optimal repression, *hr* is the DNA helical repeat, K_{max} is the association equilibrium constant for the DNA looped state at $sp_{optimal}$, and φ_{Tw} is the standard deviation of the torsion angle between operators O_{sym} and O_2 (given thermal fluctuations):

$$\varphi_{Tw}^2 = sp\left(\frac{hr}{2\pi}\right)^2 \frac{\ell k_B T}{C_{app}}$$

where ℓ is the average bp separation (3.4 Å), k_B is the Boltzmann constant, T is the absolute temperature, and C_{app} is the apparent torsional modulus for the DNA in the loop. Optimizations were performed using the SIH algorithm [12].

Supplementary References

[1] Whipple FW. Genetic analysis of prokaryotic and eukaryotic DNA-binding proteins in *Escherichia coli*. Nucleic Acids Res 1998; 26: 3700-6.

[2] Datsenko KA, Wanner BL. One-step inactivation of chromosomal genes in *Escherichia coli* K-12 using PCR products. Proc Natl Acad Sci U S A 2000; 97: 6640-5.

[3] Becker NA, Kahn JD, Maher LJ 3rd. Bacterial repression loops require enhanced DNA exibility. J Mol Biol 2005; 349: 716-30.

[4] Swint-Kruse L, Elam CR, Lin JW, Wycuff DR, Shive Matthews K. Plasticity of quaternary structure: twenty-two ways to form a LacI dimer. Protein Sci 2001; 10: 262-76.

[5] Mossing MC, Record MT Jr. Upstream operators enhance repression of the lac promoter. Science 1986; 233: 889-92.

[6] Krämer H, Niemöller M, Amouyal M, Revet B, von Wilcken-Bergmann B, Müller-Hill B. lac repressor forms loops with linear DNA carrying two suitably spaced lac operators. EMBO J 1987; 6: 1481-91.

[7] Bellomy GR, Mossing MC, Record MT Jr. Physical properties of DNA in vivo as probed by the length dependence of the lac operator looping process. Biochemistry 1988; 27: 3900-6.

[8] Oehler S, Eismann ER, Krämer H, Müller-Hill B. The three operators of the lac operon cooperate in repression. EMBO J 1990; 9: 973-9.

[9] Law SM, Bellomy GR, Schlax PJ, Record MT Jr. In vivo thermodynamic analysis of repression with and without looping in lac constructs. Estimates of free and local lac repressor concentrations and of physical properties of a region of supercoiled plasmid DNA in vivo. J Mol Biol 1993; 230: 161-73.

[10] Muller J, Oehler S, Muller-Hill B. Repression of lac promoter as a function of distance, phase and quality of an auxiliary lac operator. J Mol Biol 1996; 257: 21-9.

[11] Peters JP, Becker NA, Rueter EM, Bajzer Z, Kahn JD, Maher LJ 3rd. Quantitative methods for measuring DNA exibility in vitro and in vivo. Methods Enzymol 2011; 488: 287-335.

[12] Offord C, Bajzer Z. A hybrid global optimization algorithm involving simplex and inductive search, in: International Conference on Computational Science. Springer 2001: 680-688.

Table S1. List of bacterial strains (WT LacI unless indicated)

Assay	Spacing (bp) or Episome Identifier	WT Strain	ΔHU Strain
Growth curve	80.5	BL604	
	78.5		BL663
Chloroquine gel	80.5	BL604	
	78.5		BL663
Luciferase	p_{topA}	BL826	BL828
	p_{gyrA}	BL834	BL836
β-galactosidase	65.5	BL640	BL652
	67.5	BL580	BL654
	70.5	BL575	BL655
	72.5	BL563	BL657
	74.5	BL626	BL659
	76.5	BL592	BL661
	78.5	BL602	BL663
	80.5	BL604	BL665
	82.5	BL560	BL667
	84.5	BL596	BL669
	86.5	BL606	BL671
	88.5	BL608	BL673
	O_2 alone	BL546	BL679
	77.5, LacI Y282D	BL950	
	O_2 alone, LacI Y282D	BL1271	

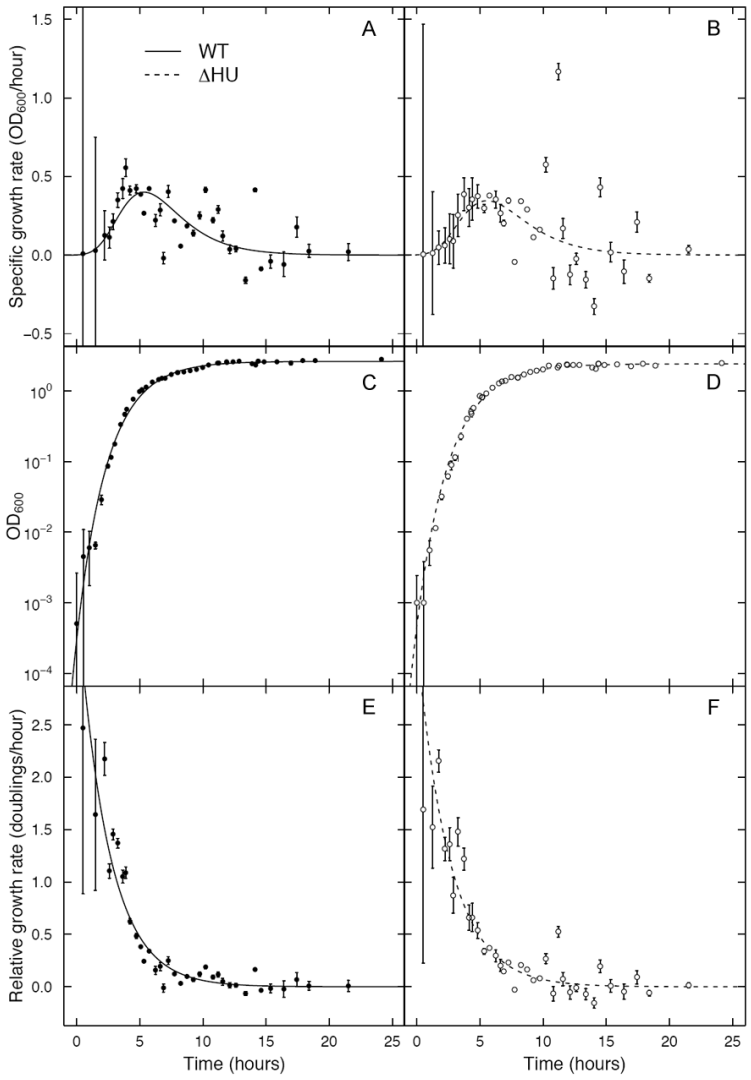

Figure S1. The specific growth rate, i.e. the first derivative (with respect to time) of the modified Gompertz growth curve (c.f. **Figure 1** of the main text), is shown for WT (A) and ΔHU (B) cells. A central difference quotient was calculated from the discrete data and error propagated to give the error bars. Growth data and modified Gompertz growth curve with OD_{600} on a logarithmic scale for WT (C) and ΔHU (D) cells. The relative growth rate, i.e. the first derivative (with respect to time) of the curves in (C and D), for WT (E) and ΔHU (F) cells. A central difference quotient was calculated from the discrete data and error propagated to give the error bars.

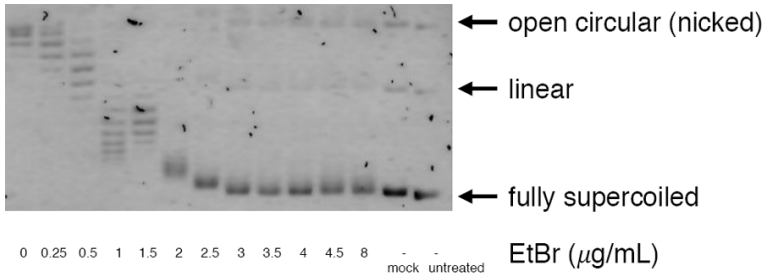

Figure S2. Purified pUC19 plasmids were relaxed by *E. coli* topoisomerase I treatment in the presence of 0-8 μg/mL of ethidium bromide (EtBr). One sample was treated in the same manner without EtBr and topoisomerase I (mock) and one sample was untreated. Each reaction generated a Gaussian distribution of topoisomers about a mean, where the EtBr concentration determined the position of the mean. The topoisomers were separated by electrophoresis through a 1% agarose slab gel. Separation was carried out at 2.5 V/cm for 21 h at 4°C in 1X TAE buffer. The gel was then stained in electrophoresis running buffer containing 0.5 μg/mL EtBr for 35 min and imaged. The labels at the right indicate the migration of open circular (nicked), linearized, and fully supercoiled plasmid.

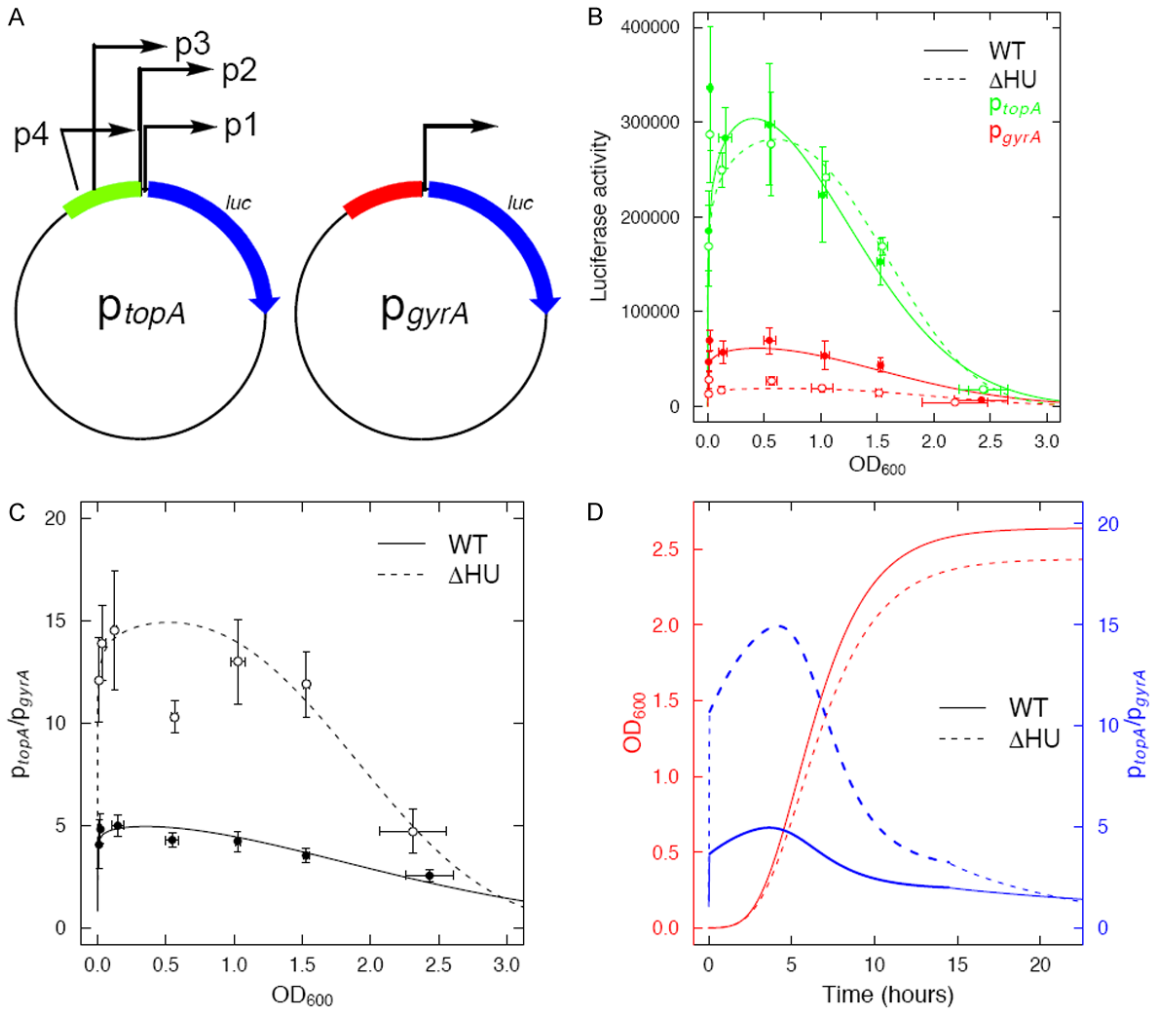

Figure S3. Unrestrained DNA supercoiling status assayed by luciferase assays. Firefly *luc* expression is driven by either the *topA* promoter cluster or the *gyrA* promoter, which are known to be sensitive to the level of unrestrained negative supercoiling. Specifically, p_{topA} is induced by high levels of negative superhelical strain (and repressed by low levels) and p_{gyrA} is induced by low levels of negative supercoiling (and repressed by high levels). (A) Constructs containing *topA* promoter cluster (green, left) or *gyrA* promoter (red, right) each with a firefly luciferase reporter gene (blue) were integrated into the large single copy F128 episome. (B) Luciferase activity data (error bars indicating standard deviation) from each of the F128 integrated reporter strains (p_{topA}, green or p_{gyrA}, red) in both WT (solid lines) and ΔHU (dashed lines) backgrounds. Curves are drawn to guide the eye. (C) Ratio of reporter activity at each growth point. The quotient of the activities (p_{topA}/p_{gyrA}) provides an estimate of the relative level of unrestrained supercoiling, which can be compared across strains. (D) Superimposition of the ratio of reporter activity (p_{topA}/p_{gyrA}) on the corresponding strain growth curves.